

Won Park and J.-B. Lee

Mechanically Tunable Photonic Crystals



The next frontier in photonic crystal research may be to achieve dynamic tunability that allows real-time, on-demand control of the photonic band structure. Recently, researchers have been working on a new strategy for achieving this goal—by applying mechanical force. This approach can produce much greater tunability than is possible with electro-optic materials and may greatly expand the usefulness of photonic crystals.



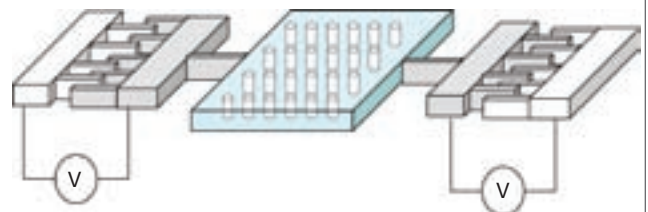
The term “photonic crystal” refers to a material that has a periodic refractive index. This periodic index profile affects the propagation of light in much the same way that the periodic potential influences electronic motion in natural crystals, leading to novel optical phenomena such as photonic band gaps, self-collimation and negative refraction. Thanks to recent progress in nanofabrication technologies, researchers can now build these structures with extreme precision.

These crystals offer great engineering freedom because their optical properties are derived from their structural design. In this respect, photonic crystals (PCs) may also be considered a form of optical metamaterial (although metamaterials are typically defined more narrowly, as a composite structure with structural units much smaller than the operating wavelength). In any case, PCs open a wealth of exciting research and engineering possibilities that may lead to new applications in thin-film optics, optical waveguiding and optical computing.

The next frontier in the photonic crystal research may be to achieve dynamic tunability that allows real-time, on-demand control of the photonic band structure. This would be a crucial improvement that could greatly expand the usefulness of PCs. Many researchers have tried using liquid crystals to achieve dynamic tunability; these crystals are relatively easy to incorporate into PC structures and allow electro-optic and thermal tuning. Busch and John predicted the tunability of the photonic band structure by infiltrating liquid crystal into an opal. In addition, much theoretical and experimental research has been done on temperature and electro-optic tuning of liquid-crystal-infiltrated PC structures.

So far, most of that work has involved shifting the photonic bandgap or defect modes using nematic liquid crystals. However, the index anisotropy Δn is about 0.2 in most liquid crystals, which is rather small. Furthermore, the infiltrated liquid crystals often occupy only a small fraction of the total volume inside the photonic crystal. A 3D modeling study that took into account the finite thickness of the slab PC structure predicted only limited tunability due to the small attainable changes in the refractive index of the liquid crystal and their small volume fraction.

[Mechanically tunable photonic crystal structure]



Mechanically tunable photonic crystal consisting of a periodic array of silicon nanorods embedded in a flexible polymer membrane. We applied mechanical force using mechanical actuators fabricated with MEMS technology.

Moreover, in most experimental realizations, the effective liquid crystal volume is further diminished by the strong surface pinning effect. While there are other possible ways to enhance the tunability (e.g., using a superlattice structure), it remains difficult to achieve wide tunability with liquid-crystal-infiltrated PCs. Other electro-optic materials, such as lead lanthanum zirconium titanate (PbLaZrTiO_3) and lithium niobate, face a similar problem and are much more difficult to process.

Recently, researchers have proposed a radically different approach to achieving tunability—by using mechanical force. The mechanically tunable PC (MTPC) structure is comprised of a periodic array of high-index dielectric materials embedded in a low-index polymer film, such as polyimide and SU8 (a standard polymer photoresist). The structure is subject to an external mechanical force by a silicon or metallic nano-/microelectromechanical system (NEMS/MEMS) actuator that stretches and releases the flexible polymer membrane. The application of mechanical force causes physical changes in the photonic crystal structure to which the photonic bands are extremely sensitive. This approach can therefore produce much greater tunability than what is possible with electro-optic materials. Possible applications include modulators, filters and on-chip sensors.

Tuning light propagation in photonic crystals

To demonstrate the tunability achievable in MTPCs, we first present numerical modeling results on the effect of mechanical force on optical beam propagation. Photonic crystals are known to exhibit anomalous refraction behavior due to the strong modification of the dispersive surface by the periodicity. This phenomenon is best illustrated by the equi-frequency contour (EFC), which refers to the locus of allowed wave vectors for a given frequency. The figure on the right shows the EFC for a triangular array of silicon pillars embedded in a flexible polymer. This structure was found to exhibit anomalous refraction behavior at a normalized frequency ($\omega a/2\pi c$) of 0.39.

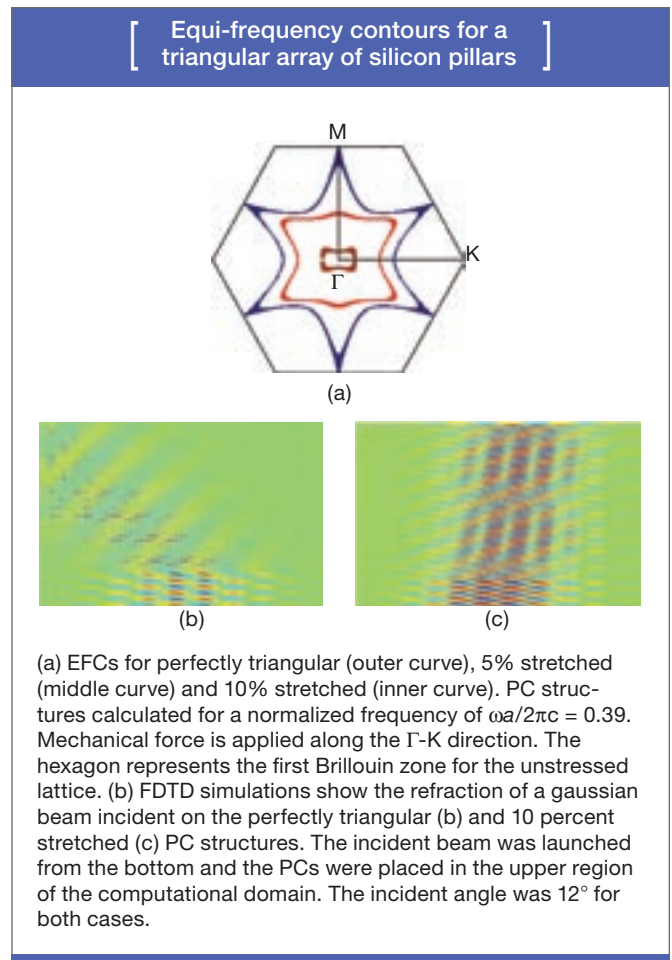
The EFC for the unstressed triangular PC had a star-like shape. It exhibited sharp inflection points along the high symmetry directions, Γ -M and Γ -K. These points represented the regions where we expected anomalous refraction. When the system was under mechanical stress, the crystal symmetry was lowered and consequently the dispersive surface was strongly modified. If the PC was uniformly stretched along the Γ -K direction, the dispersion curve became distorted.

The dispersion curves along the Γ -M direction flattened significantly as the PC was stretched along the Γ -K direction. This resulted in a very large change in the refraction behavior for optical beams propagating near the Γ -M direction. Since the group velocity was defined as the gradient of dispersion surface in k -space, we could estimate the refraction angles from the curvature of the EFC. The perfect triangular lattice exhibited giant negative refraction, in which the refraction angle reached roughly 70° for an incident angle as small as 5° .

As the PC was mechanically stretched, however, due to the flattening of the dispersion contour, the refraction angle decreased dramatically and varied only slightly as the incident angle was changed. Furthermore, for the case of 10 percent stretching, it no longer exhibited negative refraction and switched to the normal positive refraction behavior. The differences in refraction angles between the perfect triangular lattice and the 10 percent stretched crystal reached more than 75° as the incident angle was varied between 5° and 15° . This is an order of magnitude greater than what is achievable with liquid crystals, which typically exhibit at most a 15 percent change in refractive index.

We conducted two finite-difference time-domain (FDTD) simulations for a perfect triangular lattice and 10 percent stretched crystal with a Gaussian beam incident with an angle of 12° . The incident Gaussian beam was launched from the bottom of the computational domain and the MTPC structure was placed in the upper region. The large difference in refraction angles between the two cases was clearly shown.

We achieved this large change in refraction angle with a relatively small mechanical deformation. When the system is designed for the communication wavelength of $1.54 \mu\text{m}$, the pillar-to-pillar distance, a , is $0.6 \mu\text{m}$ and a 10 percent change was a mere 60 nm per unit cell. A larger stretching could, of course, induce an even greater change in refraction



behavior—but one must also consider fatigue and the elasticity limit of the polymer.

We performed finite element modeling and confirmed that, with up to 10 percent stretching, the polymer would be stretched uniformly with its displacement linearly proportional to the applied mechanical force. Another important consideration was the Poisson ratio of the flexible polymer. Polydimethylsiloxane (PDMS), for example, has a very large value of Poisson ratio, approaching nearly 0.5. This means that a 10 percent stretching along the Γ -K direction will result in a simultaneous reduction in film thickness by 5 percent, or 15 nm, in our test structure. Fortunately, the photonic band structure was not very sensitive to the slab thickness. Thus, such small changes in slab thickness will not significantly affect the light propagation characteristics.

MTPC can also be applied to negative index imaging. PCs are known to exhibit negative refraction through two different ranges of operation—near the top of the first photonic band where the EFC has negative curvature or in the second photonic band, which has a negative gradient. Recently, researchers have demonstrated negative index imaging for both cases at the telecommunication wavelength of $1.5 \mu\text{m}$ in silicon-based PC structures. Negative refraction generally exhibits acute

Recently, researchers have proposed a radically different approach to achieving tunability—by using mechanical force.



frequency dependence, placing a severe limitation on the operating frequency range.

Obviously, achieving broadband operation would greatly expand the utility of negative index materials. Recently, researchers have proposed that broadband negative index imaging with minimal chromatic aberrations can be achieved by a graded negative index PC structure. Alternatively, the MTPC concept can be used to tune the negative index and realize broadband negative index imaging.

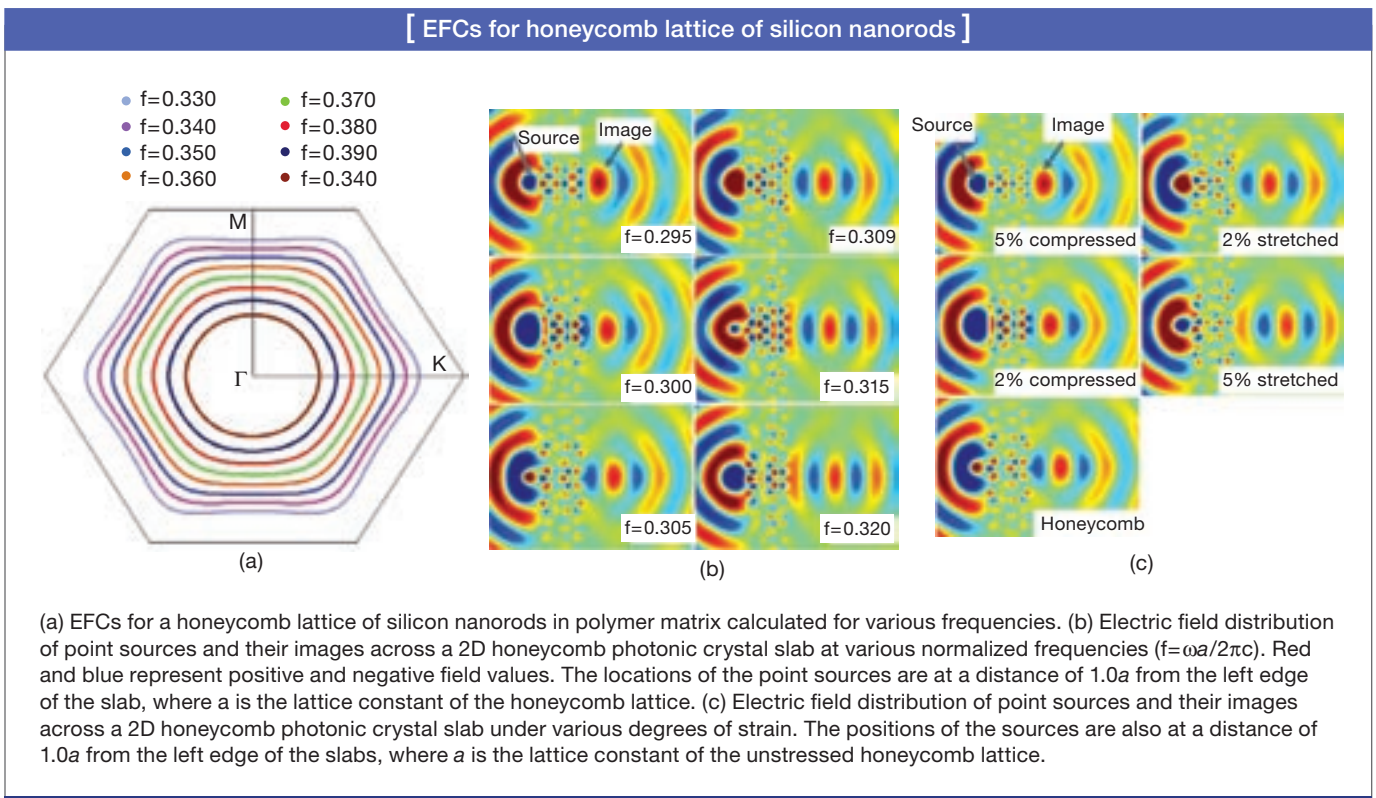
To demonstrate tunable negative index imaging, we investigated the effect of mechanical stress on a 2D honeycomb lattice of silicon rods in polyimide. In this structure, the EFCs were found to be circular near the top of the second band and gradually deformed to a hexagonal shape as the frequency was decreased.

The EFCs became smaller with increasing frequency, which is typical of the negative refraction regime. Since the effective index was measured by the radius of the EFC, it decreased in magnitude with increasing frequency. We therefore expected that the image should form farther away from the PC lens at a higher frequency. In order to directly visualize the focusing properties of the PC lens, we performed point source imaging

simulations using the FDTD method. Consistent with our analysis based on EFCs, the image did indeed move away from the lens with increasing frequency.

When we applied mechanical stress, the EFC was strongly deformed, and, consequently, the focusing characteristics were modified. In the following simulations, we assumed that mechanical stress was applied along the Γ -K direction and the dimension along Γ -M direction remained unchanged. In real space, Γ -K is the direction perpendicular to the optic axis of the PC lens and Γ -M corresponds to the direction along the thickness of the PC lens. We modeled three cases of stretching and compression by 2, 5 and 10 percent. Here, the 2 percent stretched lattice means that the distance between the two neighboring silicon pillars is 2 percent longer than that in the unstressed honeycomb lattice.

The general trend was that the image moved farther away from the PC lens as the PC structure was stretched. On the other hand, as the PC lattice was compressed, the image appeared closer to the PC slabs. The observed behavior was also consistent with the EFCs. The stretched lattices had smaller EFCs than the unstressed honeycomb PC. Conversely, the EFCs of compressed lattices were larger. A smaller EFC



corresponded to a smaller effective index. Consequently, the image should be farther away from the PC, which was exactly what we found from the FDTD simulations.

By combining the frequency dependence and the mechanical stress effect, we can develop a tunable negative index PC lens, which focuses only the desired frequency component on the detector at fixed position. The detected frequency component can be tuned by the mechanical force, enabling frequency-selective detection. We estimate that a 10 percent strain will provide a frequency bandwidth of 12.9 percent of the center frequency. This corresponds to a tunable bandwidth of 200 nm at the communication wavelength of 1.54 μm .

Demonstration of a mechanically tunable PC

In order for the MTPC to be realized, the high-index dielectric rod array embedded in a low-index polymer membrane should be flexible enough to create the structural displacement, but sufficiently stiff to ensure that the membrane does not sag and remains suspended in air. Our initial investigation began with a PDMS-based MTPC. We found this model to be infeasible: Because PDMS has an extremely low Young's modulus (below 1 MPa), the polymer membrane embedded with silicon nanorods was not stiff enough to remain suspended.

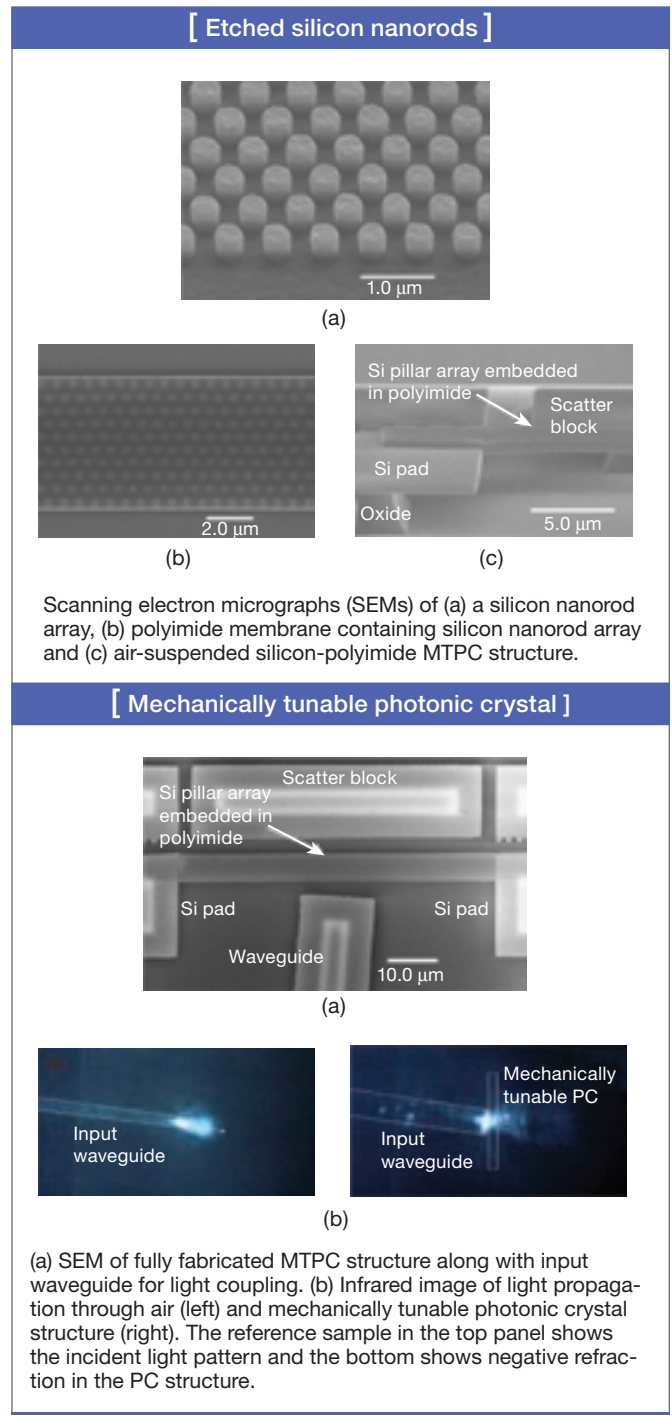
When we replaced PDMS with polyimide, which has a much higher Young's modulus (several GPa), the polymer membrane became stiff enough to remain stably suspended. The test structure consisted of a 10×100 triangular array of silicon nanorods embedded in a polyimide membrane. To observe negative refraction in the near-infrared region, around 1.5 μm , we had to make the silicon nanorods with a diameter of 400 nm and spacing of 613 nm; the total device size was $5.2 \times 61.4 \mu\text{m}$.

We fabricated the device on a 0.35- μm -thick undoped polysilicon layer on top of a 3.0- μm -thick silicon dioxide layer. A poly(methyl methacrylate) (PMMA) bi-layer copolymer photoresist stack was then exposed via electron-beam lithography to form the pattern for the silicon nanorods used to make the photonic crystal device. Then, we formed a 15-nm-thick chromium mask by the lift-off process and subsequently etched the silicon nanorods anisotropically by using the $\text{CF}_4/8.75$ percent O_2 reactive ion etch plasma (RIE).

We then deposited polyimide over the silicon nanorod array by spin coating and formed a 400-nm-thick polyimide film to totally encase the silicon nanorods. The second-level polyimide mask was formed using the same PMMA copolymer process and chromium lift-off process and etched anisotropically using 100 percent O_2 RIE.

Finally, we released the device using a buffered oxide etch methanol release process. The completed device shows the silicon-polyimide membrane after the underlying SiO_2 layer has been etched away, leaving the PC matrix intact and suspended over 3 μm of air.

For optical characterizations, we co-fabricated a 15- μm -wide input waveguide with the MTPC structure. It was wide enough



(a) SEM of fully fabricated MTPC structure along with input waveguide for light coupling. (b) Infrared image of light propagation through air (left) and mechanically tunable photonic crystal structure (right). The reference sample in the top panel shows the incident light pattern and the bottom shows negative refraction in the PC structure.

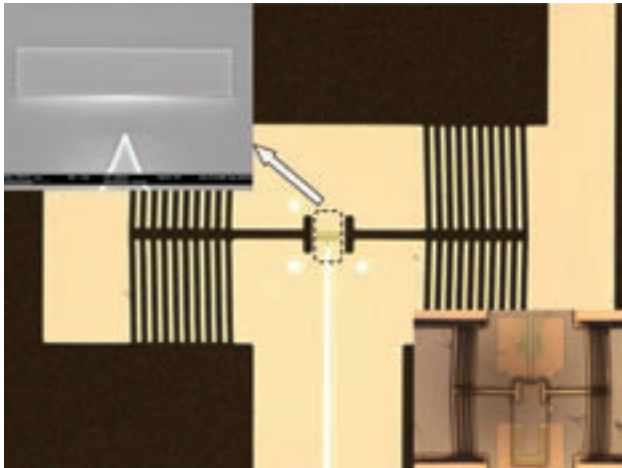
to provide a plane-wave-like incident field and make an incident angle between 2° and 10° . Light is first end-fire-coupled into the silicon ridge waveguide from a fiber pigtailed tunable diode laser operating at 1,546 nm. The scattered light is collected by an imaging system that projects the scattered image onto an infrared vidicon camera.

The plane-wave-like incident field allows us to measure the refraction angle and estimate the effective index from Snell's

Recently, researchers have proposed that broadband negative index imaging with minimal chromatic aberrations can be achieved by a graded negative index PC structure.



[The fully integrated system]



The fully integrated system showing the mechanically tunable photonic crystal structure in the center and a pair of chevron electro-thermal actuators for mechanical tuning. Top-left inset shows the SEM of the photonic crystal structure with a tapered input waveguide. Bottom-right-corner inset shows the finite element modeling of mechanical actuators.

law. As shown in part (b) of the bottom figure on p. 44, light left the ridge waveguide with the PC region absent to give the profile of the incident field. The shape of the exiting wave resembled the lowest-order transverse mode, indicating that there had been only small mode coupling that was directed parallel to the input guide.

The light path inside the PC that bent toward the upper right at an angle greater than the 6° incident wave clearly exhibited negative refraction. The optical field stayed transversely confined inside the PC and then diffracted after leaving the structure. The angle of the negative refraction showed good agreement with both the photonic band structure and the FDTD simulations.

We used a micromechanical electro-thermal actuator to apply the external mechanical force needed to mechanically tune the photonic crystal. The chevron electro-thermal actuator is an array of pre-angled narrow beams through which current flows. The finite resistance of the beams resulted in Joule heating, which in turn led to structural elongation of the beams. Since the beam arrays are joined at the center, such a structural elongation by individual beams will result in coordinated displacement at the center of the beams.

Researchers are currently working toward complete integration of a chevron electro-thermal actuator with the air-suspended polymer matrix that encases the hexagonal single crystal silicon rod array. In order to demonstrate tunable negative index imaging, the input waveguide tip was tapered and thus produced a point-source-like incident field. Finite element analysis showed that the system was mechanically stable and could be expected to produce controlled mechanical strain.

The fully integrated system will enable spectroscopic detection in a compact geometry. The process is based on silicon technology and compatible with a variety of other devices for more complex system integration. The MTPC is therefore a highly promising route for on-chip integrated sensing or detection. The ability to perform spectroscopy will greatly enhance sensitivity and specificity. This makes MTPC a highly desirable platform for sensing applications that require portable devices with high sensitivity. ▲

The authors gratefully acknowledge financial support by the National Science Foundation through grant BES-0608934 and one of us (W.P.) acknowledges the U.S. Army Research Office under MURI Contract 50432-PH-MUR.



Won Park (won.park@colorado.edu) is with the department of electrical and computer engineering, University of Colorado, Boulder, Colo., U.S.A. J.-B. Lee is with the department of electrical engineering, University of Texas, Dallas, Texas, U.S.A.

[References and Resources]

- >> K. Busch and S. John. Phys. Rev. Lett. **83**, 967 (1999).
- >> M. Notomi. Phys. Rev. B **62**, 10696 (2000).
- >> C. Luo et al. Phys. Rev. B **65**, 201104 (2002).
- >> W. Park and C.J. Summers. Opt. Lett. **27**, 1397 (2002).
- >> S. Xiong and H. Fukshima. J. Appl. Phys. **94**, 1286 (2003).
- >> W. Park and J.-B. Lee. Appl. Phys. Lett. **85**, 4845 (2004).
- >> W. Park and C.J. Summers. Appl. Phys. Lett. **84**, 2013 (2004).
- >> C.J. Summers et al. J. Nonlinear Opt. Phys. Mater. **12**, 587 (2003).
- >> E. Schonbrun et al. IEEE Photon. Technol. Lett. **17**, 1196 (2005).
- >> M. Tinker et al. J. Vac. Sci. Tech. B **24**, 705 (2006).
- >> E. Schonbrun et al. Phys. Rev. B **73**, 195117 (2006).
- >> Q. Wu et al. J. Opt. Soc. Am. B **23**, 479 (2006).
- >> E. Schonbrun et al. Appl. Phys. Lett. **90**, 041113 (2007).
- >> M. Roussey et al. J. Opt. Soc. Am. B **24**, 1416 (2007).
- >> H.-S. Kitzerow et al. Phys. Stat. Sol. (a) **204**, 3754 (2007).
- >> K. Colijnvadi et al. Microsystem Technologies **14**, 1627 (2008).
- >> Q. Wu et al. Opt. Express **16**, 16941 (2008).